Photochemical & Photobiological Sciences

Accepted Manuscript

This is an *Accepted Manuscript*, which has been through the Royal Society of Chemistry peer review process and has been accepted for publication.

Accepted Manuscripts are published online shortly after acceptance, before technical editing, formatting and proof reading. Using this free service, authors can make their results available to the community, in citable form, before we publish the edited article. We will replace this *Accepted Manuscript* with the edited and formatted *Advance Article* as soon as it is available.

You can find more information about *Accepted Manuscripts* in the Information for Authors.

Please note that technical editing may introduce minor changes to the text and/or graphics, which may alter content. The journal's standard Terms & Conditions and the Ethical guidelines still apply. In no event shall the Royal Society of Chemistry be held responsible for any errors or omissions in this *Accepted Manuscript* or any consequences arising from the use of any information it contains.

ROYAL SOCIETY OF CHEMISTRY

www.rsc.org/pps

Peptide substituted Phthalocyanine Photosensitizers: Design, Synthesis, Photophysicochemical and Photobiological Studies

Meltem Göksel[a,b], Mahmut Durmuş[b], Devrim Atilla[b*]

[a] *Kocaeli University, Kosekoy Vocational School, P.O. Box 141, Kartepe, 41135, Kocaeli, Turkey*

[b] *Gebze Technical University, Department of Chemistry, PO Box 141, Gebze, 41400, Kocaeli, Turkey*

Abstract

A series of phthalocyanine-peptide-quencher conjugates (**6-9**) were synthesized as photosensitizers for photodynamic therapy of cancer. The photophysical, photochemical and photobiological properties of these activatable molecular beacons were also investigated in this study. For this purpose, the fluorescence, singlet oxygen and photodegradation quantum yields and fluorescence lifetime values of the compounds were determined in DMSO solutions. The phototoxicity and cytotoxicity of the systems were studied against cervical cancer cell line named HeLa for their evaluation of the suitability for photodynamic therapy. The results showed that a maximum of 80% of HeLa cells were killed following light irradiation by photodynamic efficiency. All of the results showed that the novel activatable molecular beacons could be suitable candidates for cancer treatment *via* PDT technique.

Keywords: Cancer, Imaging, Targeting, Photodynamic Therapy, Matrix metalloproteinase, Quencher.

1. Introduction

Phthalocyanine-based compounds play a central role as photosensitizing agents for photodynamic therapy (PDT) of cancer *via* sensitization of tumor tissue to destruction by light. PDT relies on to benefit from improved approaches to targeting treatment. As tumors are developing, they pass through many stages that require the action of proteases. Many tumors have overexpressed the proteolytic enzymes. Studies have shown that a correlation occurs between cancer and the overexpressed proteases [1-3]. Matrix metalloproteinases (MMPs) play a major role in cell proliferation, migration, angiogenesis and apoptosis [4-6]. These enzymes are a family of zinc-dependent endopeptidases which are overexpression of MMPs promotes the spread of cancer *via* degradation of the extracellular matrix [7, 8]. It is believed that MMPs play key roles in cancer invasion and metastasis because they degraded extracellular matrix and thus malignant cells to cross the basement membrane. MMP expression is upregulated in much type of human cancers and it is associated with an aggressive tumor [5-6, 9]. These enzymes regulate a variety of physiological processes and signaling events and thus they represent key roles in the molecular communication between tumor and stroma that regulate cellular function and contribute to tumor progression. MMPs are the most important family of proteinases associated with tumorigenesis [10].

Recently, possible applications of molecular conjugates containing peptide substrate are increasing due to their disease-related target enzyme behavior [11]. Several activatable peptide-linked conjugates that simply contain either fluorophore or quencher were studied in the literature [11]. The peptide linkers in these conjugates are useful to visualize protease activities [12-22]. Peptide-based conjugates can be detected their targets *via* restoring fluorescence. These conjugates bear a photosensitizer and a quencher connected with a protease-specific peptide spacer and this system is quenched in the native state because of energy transfer between the photosensitizer and the quencher units. These conjugates become highly fluorescent after proteolysis of peptide spacer (*via* matrix metalloproteinases cleavage) by the target enzymes which are useful for imaging of tumor area. On the other hand, the photodynamic activities of these conjugates also increase due to high singlet oxygen generation by phthalocyanine unit after proteolysis of peptide spacer (Scheme 1).

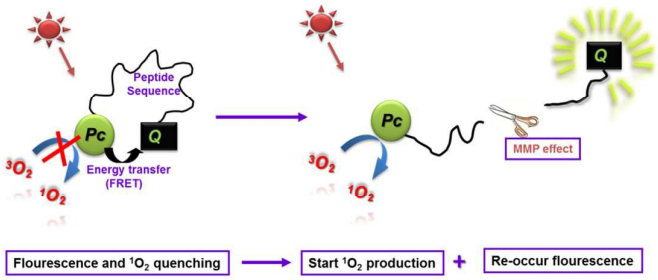

Scheme 1. Schematic illustration of activatable conjugates. Pc: phthalocyanine as a photosensitizer, Q: Quencher, MMP: matrix metalloproteinase.

Generally, the quencher efficiency of these systems depends on the type of the quenchers. Different type of quenchers can be used for the quenching mechanism. The first strategy relies on a self-quenching mechanism, in which the donor and acceptor groups are on the same or similar fluorophore molecules. These conjugates can be obtained less complicated synthesis procedures but generally they exhibit less fluorescent quenching activity. The second strategy is used an acceptor molecule which is distinct from to the donor, matching the donor fluorophore with the most efficient quencher. This strategy offers the advantage of high quenching efficiency but increases the complexity of the synthetic process. Activatable peptide-based conjugates consist of a photosensitizer and a quencher attached to opposite ends of a peptide linker [23, 24].

Activatable photosensitizers produce singlet oxygen at low quantities so they cause fewer side effects in normal cells which contain little amount of MMPs due to highly energy transfer between photosensitizer and quencher groups in normal cells. High singlet oxygen generation occurs *via* metalloproteases activation by quenched activatable photosensitizers in tumor cells that contain excessive amount of MMPs.

On the other hand, interest in fluorescence-based and other optical imaging techniques for clinical oncology has increased within the past decade. The use of cyanine dyes as contrast agents for *in vivo* optical detection of tumors has been reported by several groups [25-28]. The targeting of cyanine dyes to tumors was first achieved by using monoclonal antibodies that specifically bind to receptors on tumor cells [25, 26]. Recently, Weissleder *et al.* introduced a new targeting concept for tumor detection by developing protease-activated near-infrared fluorescent conjugates [28]. Many tumors contain overexpress receptors or other enzymes. The approach of targeting tumors by receptor-avid peptides could potentially be adapted to the optical diagnostics when the radiolabel is replaced by a fluorescent dye because fluorescence detection is highly sensitive and can detect 10^{-15} M quantities of fluorescent dyes [29].

In the present study, peptide-based activatable phthalocyanine photosensitizers bearing polyoxoethylene group were prepared for the first time (Scheme 2).

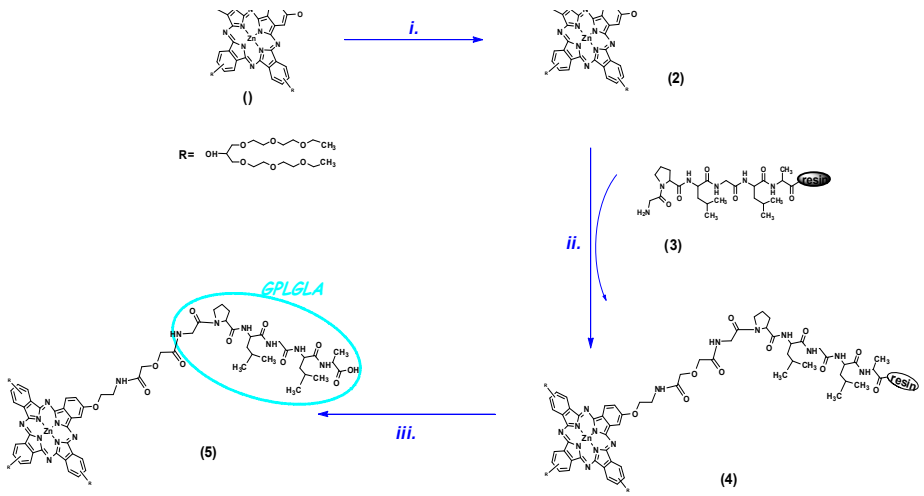

Scheme 2. The route for the synthesis of the peptide conjugated asymmetrical zinc(II) phthalocyanine conjugates. (i) diglycolic anhydride, DMF; (ii) peptide sequence on resin, HBTU, DIPEA, DMF ; (iii) TFA/TIS (95:5).

These conjugates consisted of three parts and showed multiple functions. As the first part was a asymmetric zinc(II) phthalocyanine (Pc) used as a photosensitizer, the second part was a peptide sequence which was specific for MMPs and the last part was a quencher compound. One of 2-aminopyrene (Q_1), 1-aminoquinoline (Q_2), atto 680® (Q_3) or asymmetric mono amino-functionalized zinc(II)Pc (Q_4) were used as quencher. These quencher groups with different absorption wavelengths were selected to compare their quenching efficiencies in the studied conjugates (Figure 1) .

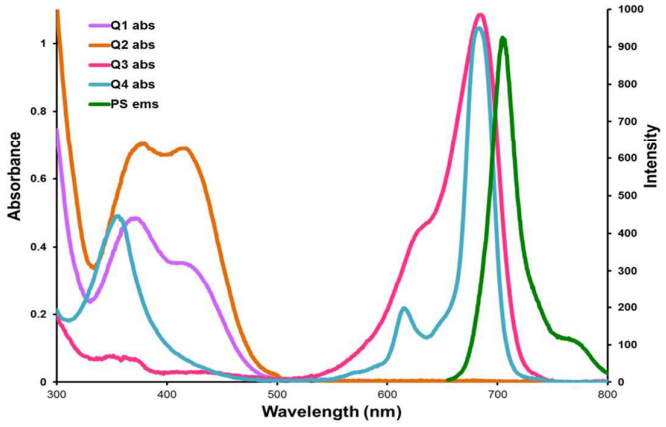

Figure 1. Electronic absorption spectra of quenchers (Q_1-Q_4) as acceptors and fluorescence emission spectrum of phthalocyanine as donor in DMSO solution.

The photophysical and photochemical properties of these conjugates (**6-9**) such as fluorescence quantum yield, lifetimes, singlet oxygen generation ability and photostability were investigated to determine of their suitability for PDT applications. In addition, the phototoxicity and cytotoxicity activities of these novel conjugates were tested against human HeLa tumor cells.

2. Experimental Section

2.1. Materials

All solvents were reagent-grade quality and obtained from commercial suppliers. 1,3-Diphenylisobenzofuran (DPBF) was obtained from Fluka. Unsubstituted zinc Pc (ZnPc)was used as standard for photophysical and photochemical measurements and it was purchased from Aldrich. *N,N*-Diisopropilethylamin (DIPEA) and O-(benzotriazol-1-yl)-*N,N,N,N*-tetramethyluronium hexafluorophosphate (HBTU) were purchased from Merck and Sigma-Aldrich, respectively. Wang resins and all of the *N*-R-fmoc-protected amino acids were also purchased from Sigma-Aldrich. All reactions were monitored by thin layer chromatography (TLC) using 0.25 mm silica gel plates (60 F_{254}) with UV indicator. Column chromatography was performed on silica gel 60 (0.04–0.063 mm) and preparative thin layer chromatography was also performed on silica gel 60 PF_{254} for the purification of the compounds.

2.2. Equipments

Elemental analyses were obtained from Thermo Finnigan Flash 1112 Instrument. Infrared spectra were recorded on a Perkin Elmer Spectrum 100 spectrophotometer. Electronic absorption spectra were measured on a Shimadzu 2101 UV-vis spectrophotometer. Fluorescence excitation and emission spectra were recorded on a Varian Eclipse spectrofluorometer using 1 cm path length cuvette at room temperature. ^{1}H NMR spectra with tetramethylsilane (TMS) as the internal standard were recorded on a Varian 500 MHz spectrometer. Chemical shifts (δ) were given in ppm relative to DMF-d_7 (8.01 ppm). The mass spectra were obtained on a BRUKER Microflex LT by MALDI (Matrix Assisted Laser Desorption Ionization)-TOF using 2,5-dihydroxybenzoic acid (DHB) as the matrix. The HPLC system was performed on an Agilent 1100 series HPLC system (ChemStation software) equipped with a G 1311A pump and G1315B diode array

detector monitoring the range 254-900 nm. A reverse phase column Shim-pack ODS (4.0 mm I.D. x 250 mm L.) (Schimadzu, Japan) was used (HPLC method; gradient solvent mixture 98% of A (0.1% TFA and 99.9% acetonitrile) and 2% of B (methanol) over 20 min; flow rate, 5.0 µL/min).

2.3. Photophysical and photochemical parameters

The used photophysical and photochemical parameters and formulas were supplied as supplementary information.

2.4. Synthesis

Asymmetrically mono-amine functionalized Zn(II)Pc (**1**) was synthesized and purified according to our previously study [30].

2.4.1. Monocarboxy functionalized asymmetric Zn(II)Pc (2)

50 mg, (0.031 mmol) mono-amine functionalized Zn(II)Pc (**1**) in 1 mL DMF was added to 7.2 mg (0.062 mmol) diglycolic anhydride and this mixture was stirred 48 hours at room temperature. The resulting mixture was extracted by liquid-liquid extraction with ethyl acetate and water. Ethyl acetate phase was dried using anhydrous Na_2SO_4 and solvent was removed under reduced pressure. The purity of the product was checked by TLC. The desired product (**2**) was dried under vacuum. Yield: 45 mg (90%). FT-IR (ν_{max}/cm^{-1}): 3438 (OH), 3077 (Aromatic-CH), 2922-2857 (Aliphatic-CH), 1721 (C=O), 1607 (C=C), 1487 (NH), 1392 (Aliphatic-CH), 1089 (C-O-C) and 1045 ([(C-(C=O)-O-(C=O)-C]). UV–vis (DMSO): λ_{max} nm (log ε) 358 (4.61), 615 (4.20), 685 (4.71). ^{1}H NMR (DMF-d_7): δ = 0.87-1.03 (m, 18H, CH_3), 3.26-3.35 (m, 24H, CH_2), 3.36-3.38 (m, 2H, CH_2N), 3.47-3.56 (m, 24H, CH_2), 3.59-3.74 (m, 24H, CH_2), 3.77-3.87 (br, 3H, CH), 3.90-3.97 (br, 6H, CH_2O), 7.10-7.81 (m, 8H, ArCH), 7.80-7.82 (br, 2H, OH and NH), 8.94-9.27 (m, 4H, ArCH). Calcd. for $C_{83}H_{115}N_9O_{26}Zn$: 57.95 C%, 6.74 H%, 7.33 N%, Found: C%, 58.52; H%, 6.75; N%, 7.68. MS (MALDI-TOF) *m/z*: Calc.: 1720.23; Found: 1721.63 $[M+H]^+$.

2.4.2. Peptide sequence (3)

The MMP-cleavable peptide sequence GPLGLA-Wang resin (**3**) [31] was prepared on 0.2 mmol scale using the fmoc strategy of solid-phase peptide synthesis (SPPS) with commercially available *N*-R-fmoc-protected amino acids. Wang resin and HBTU/DIPEA

were used as a solid support and carboxyl-group activating agents, respectively. A two-fold excess of the fmoc-protected amino acids were coupled to the Wang resin. After the final coupling, the last fmoc group was removed from the peptide-resin using 20% piperidine in N-methyl-2-pyrrolidone (NMP). The resin was washed with NMP and dichloromethane for removing of the fmoc group from the mixture.

For the characterization of obtained peptide sequence, a portion of this peptide (**3**) was treated with 95% trifluoroacetic acid (TFA) and 5% triisopropylsilane (TIS) for 1 h at room temperature to cleave the peptide sequence from the Wang resin. After removing the cleaved solid resin by filtration, the filtrate was concentrated and precipitated by adding anhydrous diethyl ether. The white solid product was obtained with good yield (80%). The purity of the obtained peptide was checked by HPLC using acetonitrile containing 0.1% TFA/MeOH (98:2) solvent system and only one peak was observed at 13"94'. FT-IR (ν_{max}/cm^{-1}): 3304 (OH), 2962-2852 (Aliphatic CH), 1643 (C=O), 1539 (C=C), 1455 (NH), 1261 (CH), 1094 (C-O-C), 1024 (CH_2-O). Calcd. for $C_{24}H_{42}N_6O_7$: 54.74 C%, 8.04 H%, 15.96 N%, Found: C%, 54.52; H%, 8.75; N%, 16.08. This peptide was also characterized by MS (MALDI-TOF) *m/z*: Calc.: 526.62; Found: 527.77 $[M+H]^+$.

2.4.3. Pc-peptide conjugate (5)

Monocarboxy functionalized Zn(II)Pc (**2**) (20 mg; 0.012 mmol) was dissolved in 1 mL DMF. Dicyclohexylcarbodiimide (DCC) (3.6 mg; 0.017 mmol) and N-hydroxysuccinimide (NHS) (2 mg; 0.017 mmol) were added to the solution of the Pc (**2**) and stirred 10 minutes to activation of carboxyl group. At the end of this time, the peptide sequence (**3**) (6.1 mg; 0.012 mmol) contains free N-terminal amino group swelled in DMF for 1 hour and it was added to the reaction mixture and this mixture was also stirred further 24 hours at 30°C. After this time, the reaction mixture washed with MeOH (2x20 mL) and CH_2Cl_2 (2x30 mL) to remove unreacted phthalocyanine **2**. Phthalocyanine-peptide conjugate (**4**) was treated with 5 mL of a mixture of TFA/TIS/H_2O (93:5:2) at room temperature for 4 hours for cleavage of the solid resin. The resin was filtered, washed with TFA (3x2 mL), the filtrates were combined and evaporated under vacuum to give green targeted compound **5**. The obtained conjugate was purified by column chromatography over Bio-Beads® S-X beads using CH_2Cl_2/C_2H_5OH (1:1) as eluent. The purity of the conjugate **5** was controlled by reverse-phase HPLC on a Luna C18 semi-preparative column (10x250 mm, 5 μm) (Phenomenex, U.S.A.) using a solvent system of water and acetonitrile both containing 0.1% TFA, with a stepwise gradient from

50% to 95%. The purity of the Pc-peptide conjugate **5** was found >95%. Yield 5 mg (25%). FT-IR spectrum (ν_{max}/cm^{-1}): 3297 (OH), 3069 (Aromatic-CH), 2958-2853 (Aliphatic-CH), 1648 (C=O), 1545 (C=C), 1457 (NH), 1263 (CH), 1202 (C-N), 1137 (C-O-C). UV–Vis (DMSO): λ_{max} nm (log ε) 360 (4.40), 620 (3.98), 687 (4.71). ^{1}H NMR (DMF-d_7): δ = 0.70-0.79 (m, 33H, CH_3), 1.08-1.19 (bs, 2H, CH), 1.31-1.44 (m, 6H, CH_2), 1.68-1.81 (m, 4H, CH_2), 3.37-3.43/3.53-4.27 (m, 72H, CH_2-O), 3.45-3.52 (m, 8H, CH_2), 4.28-4.33 (m, 4H, CH_2), 4.33-4.38 (m, 7H, CH), 11.66-11.95 (br, 6H, NH), 12.15-12.29/12.37-12.53/12.62-12.91 (m, 12H, ArH), 12.93-13.16 (br, 1H, OH). Calcd. for $C_{107}H_{155}N_{15}O_{32}Zn$: C%, 57.89; H%, 6.97; N%, 9.38. Found: C%, 57.52; H%, 7.25; N%, 9.68. MS (MALDI-TOF) *m/z*: Calc.: 2228.88; Found: 2269.803 $[M+K+2H]^+$.

2.4.4. Conjugates (6-9).

The Pc-peptide conjugate (**5**) (10 mg; 4.3 μmol) was dissolved in 500 μl of DMF. DCC (1.33 mg; 6.5 μmol) and NHS (0.74 mg; 6.5 μmol) were added to this mixture and then stirred for 2 hours at 50°C for activating carboxyl group. After then, the mixture was reacted with 4.3 μmol quencher such as 6-aminoquinoline (0.62 mg), 1-aminopyrene (0.93 mg), Atto-680® (2.24 mg) or asymmetrically mono amino functionalized ZnPc (**1**) (6.89 mg). After this time, the reaction mixture was precipitated by the addition of 2 mL of hexane and Pc-peptide-quencher conjugates were obtained. The crude products were purified by column chromatography over Bio-Beads® S-X beads using CH_2Cl_2 as eluent. The green solid products were obtained to yield 7.4 mg (74%), 7.22 mg (72%), 7.58 mg (75%), and 7.16 mg (71%) for conjugates **6**, **7**, **8**, and **9**, respectively.

Conjugate 6: FT-IR (ν_{max}/cm^{-1}): 3311 (NH), 3088 (Aromatic-CH), 2965-2878 (Aliphatic-CH), 1660-1627 (C=O), 1572-1540 (C=C), 1438 (NH), 1243 (CH), 1088 (C-O-C). UV–vis (DMSO): λ_{max} nm (log ε) 358 (4.25), 620 (3.86), 685 (4.51). ^{1}H NMR (DMF-d_7): δ = 0.82-0.91 (m, 12H, CH_3), 0.98-1.22 (m, 18H, CH_3), 1.23-1.32 (m, 3H, CH_3), 1.42-1.49 (m, 2H, CH), 2.09-3.13 (m, 10H, CH_2), 3.42-3.92 (m, 72H, CH_2), 4.08-4.29 (m, 12H, CH_2), 4.40-4.53 (m, 4H, CH), 4.55-4.62 (m, 3H, CH), 6.83-7.49 (m, 18H, ArH), 7.93-8.12 (m, 7H, NH). Calcd. for $C_{116}H_{161}N_{17}O_{31}Zn$: C%, 59.16; H%, 6.89; N%, 10.11. Found: C%, 59.52; H%, 6.75; N%, 10.68. MS (MALDI-TOF) *m/z*: Calc.: 2354.99; Found: 2378.32$[M+Na]^+$.

Conjugate 7: FT-IR (ν_{max}/cm^{-1}): 3380 (NH), 3051 (Aromatic-CH), 2928-2876 (Aliphatic-CH), 1664 (C=O), 1609 (C=C), 1493 (NH), 1238 (CH), 1024 (C-O-C). UV–vis (DMSO): λ_{max} nm (log ε) 359 (4.25), 612 (3.86), 686 (4.52). ^{1}H NMR (DMF-d_7): δ = 0.98-

1.38 (m, 33H, CH_3), 1.40-1.45 (m, 2H, CH), 1.82-2.03 (m, 6H, CH_2), 2.56-3.40 (m, 4H, CH_2), 3.55-4.12 (m, 72H, CH_2), 4.13-4.45 (m, 12H, CH_2), 4.52-4.72 (m, 7H, CH), 7.59-7.92 (m, 12H, ArH), 7.83-8.01 (m, 7H, NH), 8.04-8.20 (m, 9H, ArH). Calcd. for $C_{123}H_{164}N_{16}O_{31}Zn$: C%, 60.84; H%, 6.81; N%, 9.23. Found: C%, 60.93; H%, 6.91; N%, 9.55. MS (MALDI-TOF) *m/z*: Calc.: 2428.10; Found: 2453.64 $[M+Na+H]^+$.

Conjugate 8: FT-IR (ν_{max}/cm^{-1}): 3325 (NH), 3079 (Aromatic-CH), 2931-2852 (Aliphatic-CH), 1660-1626 (C=O), 1572-1539 (C=C), 1438 (NH), 1244 (CH), 1089 (C-O-C). UV–vis (DMSO): λ_{max} nm (log ε) 354 (4.24), 619 (3.87), 685 (4.56). ^{1}H NMR (DMF-d_7): δ = 0.75-1.03 (m, 15H, CH_3), 1.18-1.39 (m, 18H, CH_3), 1.46-1.54 (m, 9H, CH_3), 1.56-1.62 (m, 2H, CH), 2.16-3.35 (m, 22H, CH_2), 3.39-4.26 (m, 72H, CH_2), 4.29-4.43 (m, 18H, CH_2), 4.45-4.50 (m, 5H, CH), 6.34-6.56 (m, 5H, ArH), 7.03-7.53 (m, 12H, ArH), 7.92-8.33 (b, 7H, NH). Calcd. for $C_{134}H_{185}N_{19}O_{36}SZn$: C%, 58.84; H%, 6.82; N%, 9.73. Found: C%, 59.02; H%, 6.75; N%, 9.68. MS (MALDI-TOF) *m/z*: Calc.: 2735.46.; Found: 2777.23 $[M+K+H]^+$.

Conjugate 9. FT-IR (ν_{max}/cm^{-1}): 3506 (NH), 3076 (Aromatic-CH), 2929-2907 (Aliphatic-CH), 1692 (C=O), 1610 (C=C), 1491 (NH), 1398 (CH), 1264 (Aromatic-CH), 1101 (C-O-C). UV–vis (DMSO): λ_{max} nm (log ε) 358 (5.09), 615 (4.45), 687 (5.10). ^{1}H NMR (DMF-d_7): δ = 0.90-1.19 (m, 48H, CH_3), 1.32-1.43 (m, 3H, CH_3), 1.48-1.51 (m, 8H, CH), 1.71-1.94 (m, 6H, CH_2), 2.24-3.51 (m, 122H, CH_2), 3.53-4.02 (m, 24H, CH_2), 4.05-4.25 (m, 8H, CH_2), 4.28-4.42 (m, 10H, CH_2), 4.53-4.68 (m, 4H, CH), 6.89-8.20 (m, 31H, ArH/NH). Calcd. for $C_{186}H_{264}N_{24}O_{53}Zn_2$: C%, 58.56; H%, 6.97; N%, 8.81. Found: C%, 58.02; H%, 6.92; N%, 8.73. MS (MALDI-TOF) *m/z*: Calc.: 3815.00.; Found: 3649.81 $[M-11CH_3]$ and 3842.39 $[M+Na+4H]^+$.

2.5. Biological studies

2.5.1. Cell Culture

All tissue culture media and reagents were obtained from PAN Biotech. Human HeLa cells were cultured in DMEM supplemented with 10% fetal bovine serum, antibiotics (penicillin-streptomycin) and incubated at 37°C in a humidified atmosphere of 5% CO_2 in air. The cells were regularly sub-cultured according to their growth rate.

2.5.2. Light source

The Lumacare Model LC-122 consists of two main parts: a Quartz halogen lamp light source (100 W) housing with a control panel and power supply, and a fiber-optic probe (FOP) adaptors with filters designed to meet any optical protocol ranging from 380 to 750 nm was

used for irradiation of cells. The fiber-optic probes of the LC-122 offer output power from 10 $mW.cm^{-2}$ up to 1 $W.cm^{-2}$ at their output tips depending on filter transmission wavelength. For illumination protocol, FOP system was used with activation wavelength of 680 ± 10 nm. The exposure area was 50x75 mm and the distance between FOP tip and the cell plate surface was 20 cm. The light power of FOP systems on the exposure area was measured with a power meter that comprises from silicon detector (Ophir). The exposure energy is controlled from the control panel by a timer.

2.5.3. Cytotoxicity studies.

The HeLa cells were prepared as described above. Exponentially growing cells seeded onto 96-well plates at 4000 cells per well and allowed 24 h to attach. Various concentrations of Pc-peptide-quencher conjugates were added to exponentially growing cells and the cells were irradiated with laser irradiation after 24 hour incubation. For dark cytotoxicity experiments, conjugates (**6-9**) were added to triplicate wells in 0.5; 1; 2; 4; 6; 8 and 10 μM final concentration and the cells including these compounds were incubated for 24 hours. The compounds were replaced with fresh medium. And then, cytotoxicity was measured using tetrazolium compound reagent (WST-1, Roche) for the quantification of cell proliferation and cell viability. It is a colorimetric assay and based on the cleavage of the tetrazolium salt WST-1 by mitochondrial dehydrogenases in proliferating cells.

To each well, 20 μL of WST-1 compound was added and the plate was incubated for 4 h before reading. WST-1 tetrazolium compound is metabolized by metabolically active cells into a colored formazan product that can be measured by reading the absorbance at 450 nm with a microplate reader. The average of the triplicate wells for each sample was calculated.

2.5.4. Photo-toxicity studies.

For the photo-toxicity experiments, the HeLa cells were prepared as described above and they treated with the 0.5; 1; 2; 4; 6; 8 and 10 μM concentrations of conjugates (**6-9**) and incubated for 24 hours. After compound loading, the medium was removed and replaced with fresh medium. The cells were exposed to the light from FOP systems with activation wavelength of 680 nm for determination of photo-toxicity. The total light dose was used as 1 and 2 Jcm^{-2}. After illumination, the cells were incubated for 24 hours and then 96 well plates were measured by reading optical density at 450 nm by the Universal Microplate Reader. After incubation, the optical densities were measured using WST-1 compound as mentioned above.

3. Results and Discussion

3.1. Molecular design and synthesis

In the prepared novel molecular beacons, the Zn(II)Pc (**2**) was employed as the photosensitizing agent. The bulky polyoxoethylene glycol chains on the Pc framework were preferred to diminish aggregation tendency of the systems as well as enhance the amphiphilicity of the conjugates. The peptide sequence and the Pc ring were linked *via* peptide bond between -CO_2H group on the Pc core and -NH_2 group on the peptide sequence. The peptide sequence consisting of GPLGLA amino acids was prepared as a substrate to MMPs overexpressed enzymes by cancer cells. The used peptide sequence can be increased the accumulation of conjugate systems around the cancer cells. The synthesis of peptide sequence was shown in figure 2.

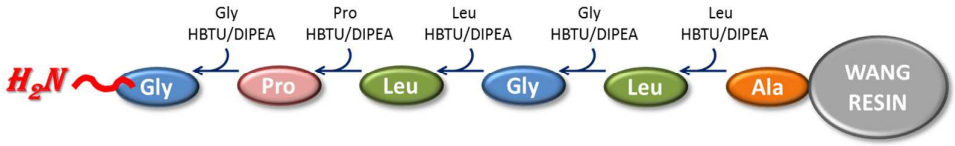

Figure 2. The synthesis route of peptide sequence via SPSS protocol.

Four different quenchers were attached to this conjugate for preparation of target molecular beacons (**6-9**). The synthetic routes for the preparation of the conjugates were shown in Schemes 2 and 3. For the synthesis of designed conjugate systems; firstly, mono-amino functionalized asymmetric Zn(II)Pc (**1**) was treated with diglycolic anhydride under appropriate conditions [25] to obtain the terminal monocarboxy functionalized Zn(II)Pc (**2**) derivative. NH_2-GPLGLA-Wang resin (**3**) was prepared by manually according to standard 9-fluorenylmethoxycarbonyl (fmoc) solid-phase-peptide synthesis (SPSS) protocol [32] using a Wang resin as a solid phase (Fig. 2) and commercially available fmoc-N-protected amino acids. Then the Pc-GPLGLA-Wang resin conjugate (**4**) was synthesized by the reaction of the Pc **2** which contains –CO_2H group with N-terminus peptide sequence of **3**. This conjugate (**4**) was cleaved from the Wang resin and Pc-peptide conjugate (**5**) was obtained. Finally, targeted Pc-peptide-quencher conjugates (**6-9**) were obtained by the formation of amide bond between the –CO_2H group on the C-terminal alanine of Pc-peptide conjugate **5** and the -NH_2 group on used quenchers (Schemes 2 and 3).

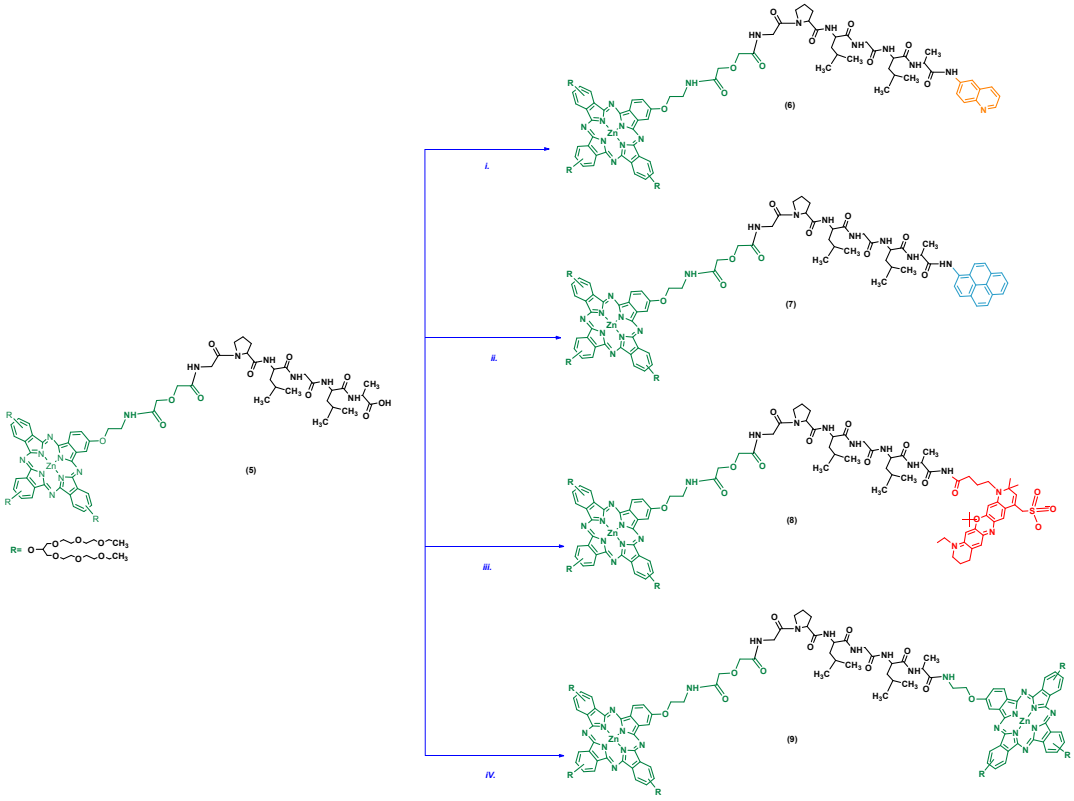

Scheme 3. The route for the synthesis of conjugates **6-9**. (i) 6-Aminoquinoline, DCC, NHS, DMF; (ii) 1-Aminopyrene, DCC, NHS, DMF; (iii) Atto 680®, DCC, NHS, DMF; (iv) Phthalocyanine **1**, DCC, NHS, DMF.

3.2. Characterization

The purity of the synthesized peptide sequence (**3**) was confirmed by HPLC and it was characterized by MALDI-TOF and FT-IR techniques (Figure 3).

Newly synthesized mono-carboxy functionalized Zn(II)Pc (**2**), Pc-peptide conjugate (**5**), and molecular beacons (**6-9**) were characterized by different analysis methods such as ^{1}H NMR, MALDI-TOF, UV-vis and FT-IR. The purity of the conjugate **5** was also confirmed by reverse phase HPLC. The newly synthesized conjugates (**6-9**) were prepared using different quenchers in order to compare the effects on photophysical, photochemical and photobiological properties of the conjugates. For this purpose, the Pc-peptide conjugate **5** was coupled to four different amino functionalized quenchers.

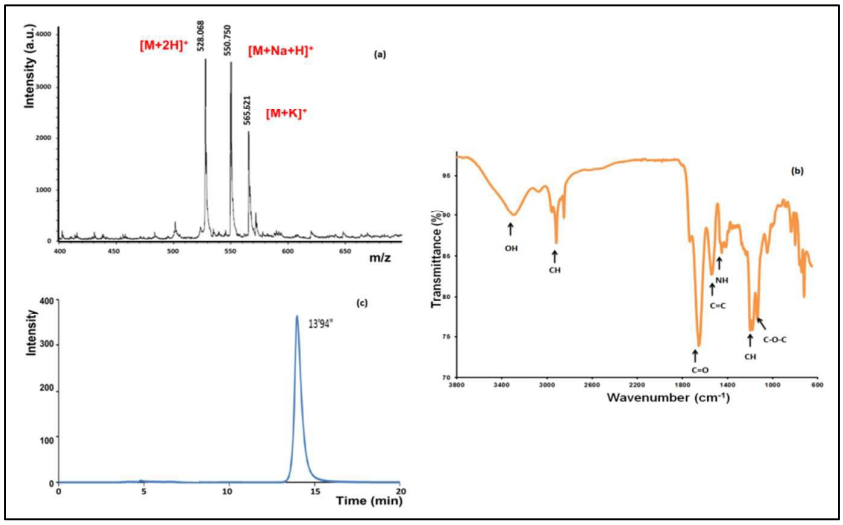

Figure 3. a) MALDI-TOF, b) FT-IR and c) HPLC spectra of synthesized peptide sequence (**3**).

These quenchers were conjugated to deprotected C-terminal alanine of **5** to obtain conjugates **6**, **7**, **8**, and **9** containing 6-amino-quinoline, 1-amino-pyrene, atto-680® and Pc **1**, respectively. The target Pc-peptide-quencher conjugates were characterized by spectroscopic techniques such as MALDI-TOF, UV-vis and FT-IR (Figure 4).

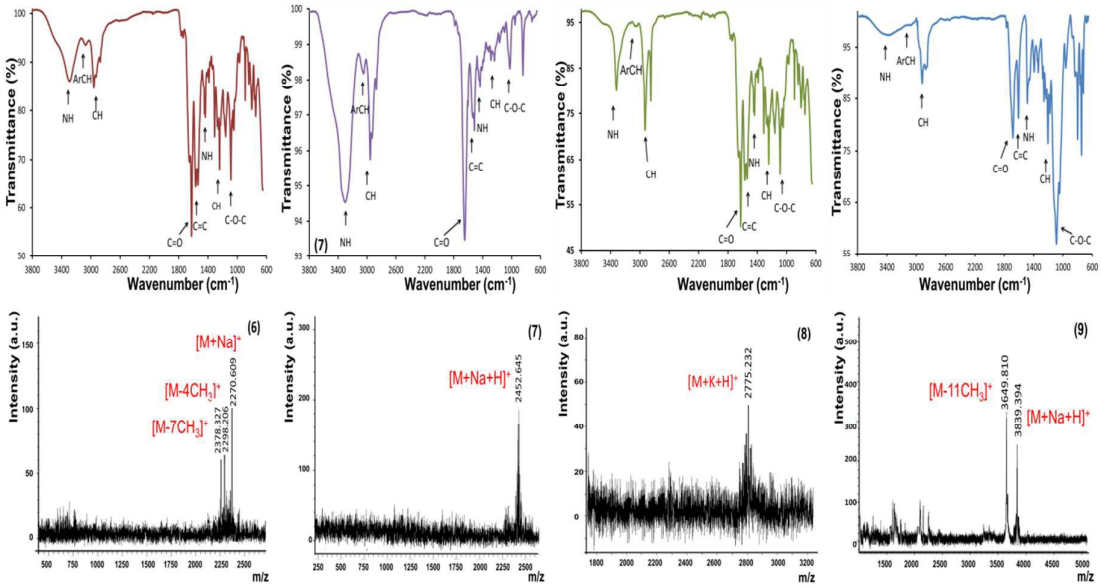

Figure 4. FT-IR and MALDI-TOF spectra of conjugates **6-9**.

In the FT-IR spectrum of compound **2**, the specific peaks belonging to anhydride group were observed at 1607 and 1721 cm^{-1} after reaction of mono-amino functionalized Pc (**1**)

with diglycolic anhydride. In the FT-IR spectrum of compound **5**, a characteristic peak at 1648 cm^{-1} was related to peptide sequence.

The FT-IR spectra of the Pc-peptide-quencher conjugates (**6**, **7**, **8**, and **9**) strongly evidenced the substitution of different fluorophore groups on the Pc core. After the conjugation reaction, the vibration peaks belonging to NH groups which indicated the formation of amide bound appeared in the FT-IR spectra. Zn(II) Pc **6**, **7**, **8** and **9** showed very similar FT-IR spectra as expected.

In the ^{1}H-NMR spectra of the Zn(II)Pc-peptide derivative (**5**) and its conjugates with quenchers (**6**, **7**, **8**, and **9**), the aromatic protons were observed between 7.18-8.02 ppm for Zn(II)Pc-peptide derivative (**5**), 7.95-8.11 ppm for conjugate **6**, 6.80-8.01 ppm for conjugate **7**, 7.59-8.24 ppm for conjugate **8** and 6.22-7.74 ppm for conjugate **9**.

In the MALDI-TOF mass spectra, the molecular ion peaks for Pc-peptide-quencher conjugates (**6**, **7**, **8**, and **9**) were observed at *m/z* = 2270.60 $[M+Na]^+$, 2448.84 $[M-CH_3]^+$, 2535.60 $[M]^+$, and 2865.03 $[M+Na]^+$, repectively. These *m/z* values were consistent with the expected structures of the target conjugates **6**, **7**, **8** and **9**.

3.3. Ground state electronic absorption spectra

The electronic absorption behaviors of terminal $–CO_2H$ containing Zn(II)Pc (**2**), Pc-peptide conjugate (**5**) and Pc-peptide-quencher conjugates (**6-9**) were determined by UV-vis spectroscopy. Generally, Pc compounds show two dominant absorption bands at visible and ultraviolet regions in their ground state electronic absorption spectra. These absorption bands are known as Q and B bands. The Q band was observed at around 600-750 nm due to the $\pi \rightarrow \pi^*$ transitions from the highest occupied molecular orbital (HOMO) to the lowest unoccupied molecular orbital (LUMO) of the Pc ring and B band was observed at around 300-450 nm arising from deeper π levels $\rightarrow$ LUMO transition.

The electronic absorption spectra of the Pcs showed monomeric behavior in DMSO evidenced by a single (narrow) Q band in the visible region (Figure 5a). The observed spectra were typical for metallated Pc complexes bearing different substituents and central metals [33]. The novel Pc **2** and **5** showed similar UV-vis spectra and Q bands were observed at 685 nm and 687 nm, respectively. The Q bands were observed at 685 nm, 686 nm, 685 nm and 682 nm for conjugates **6**, **7**, **8** and **9** in DMSO, respectively. Kind of the used the quenchers did not shown significant effect on the electronic spectra of studied conjugates **6**, **7**, **8** and **9** because the quenchers were far from the Pc core. The electronic absorption spectra of studied

Zn(II)Pc compound (**2**), Pc-peptide conjugate (**5**) and conjugates (**6-9**) were also measured in different solvents (Figure 5a as an example for compound **5**). All of studied compounds exhibited similar spectra in toluene, THF, ethanol, DMF, chloroform and DMSO. The spectra showed a single (narrow) Q bands which were evidence of monomeric behavior in the all solvents. The Q bands of the studied Pcs were 10-15 nm red-shifted when compared to ZnPc (λ= 672 nm) [34] in DMSO due to the substitution effect. On the other hand, all studied compounds showed a broad band at around 630 nm because of aggregation in water (Figure 5b as an example for compound **5**). The addition of the triton X-100 which is a surfactant for reduce aggregation for phthalocyanine compounds to the water solution of these compounds gave a monomeric single narrow Q band due to breaking of formed aggregates.

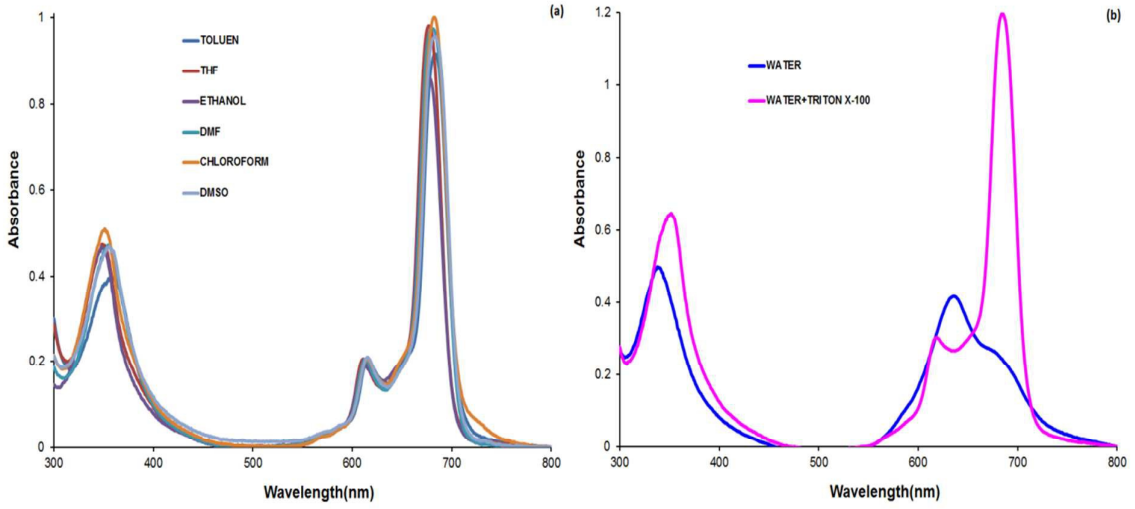

Figure 5. UV-vis absorption spectra of compound **5** (a) in different solvents and (b) water and addition of triton X-100 to water solution. Concentration= $1.00x10^{-5}$ M.

3.4. Aggregation Studies

In this study, the aggregation behavior of the Zn(II)Pc **2**, Pc-peptide conjugate (**5**) and conjugates (**6-9**) were also investigated at different concentrations in DMSO (Fig. 6 as an example for compound **8**). The Lambert–Beer law was obeyed for all of these compounds at concentrations ranging from $1.2x10^{-5}$ to $2x10^{-6}$ M. All the studied compounds did not show aggregation at the working concentration range in DMSO.

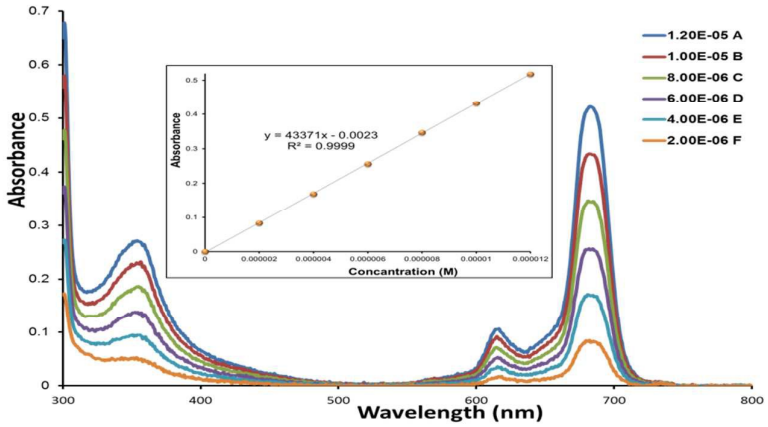

Figure 6. Absorbance changes of **8** in DMSO at different concentrations: $12x10^{-6}$ (A), $10x10^{-6}$ (B), $8x10^{-6}$ (C), $6x10^{-6}$ (D), $4x10^{-6}$ (E), $2x10^{-6}$ (F) M. (Inset: Plot of absorbance versus concentration).

3.5. Fluorescence spectra

Fluorescence spectra of the Pc derivatives (**2, 5, 6-9**) were carried out in DMSO. The fluorescence excitation and emission spectra of these compounds were typical of metal Pc complexes in DMSO. The excitation spectra were similar to absorption spectra and both of them were mirror images of the fluorescent spectra for the compounds suggesting that the molecules did not show any degradation during excitation (Fig. 7 as an example for compound **7**). Fluorescence emission maxima were observed at 692 nm for **2**, 695 nm for **5**, 693 nm for **6**, 694 nm for **7**, 699 nm for **8** and 696 nm for **9**. The Stokes' shifts ($\lambda_{ems}-\lambda_{exc}$) ranging from 6 to 14 nm for studied compounds.

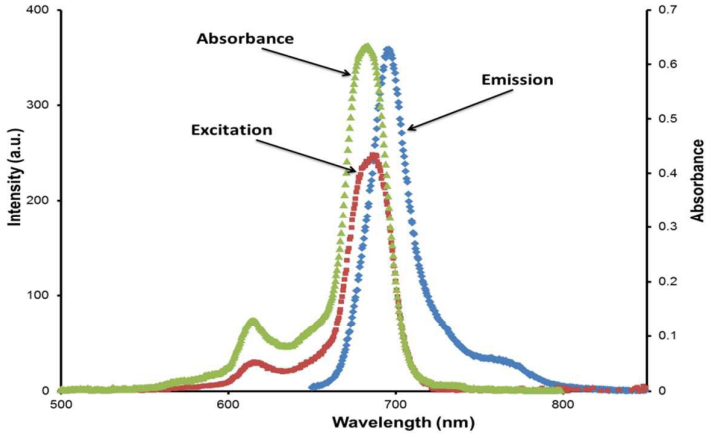

Figure 7. Absorption, excitation and emission spectra for **7** in DMSO. Excitation wavelength=650 nm.

Quencher molecules were used to enable the formation of energy transfer in designing Pc-peptide-quencher conjugates. The chemical structures, the absorption spectra of four different quenchers and the emission spectrum of the peptide conjugated Zn(II)Pc (**5**) were

supplied in Table 1 for comparing. In theory, for the formation of non-radiative-energy-transfer (quenching) between quencher and donor, the absorption spectrum of the quencher should overlap the emission spectrum of the donor. However, Lovell et al. [35], based on their study in 2009, suggested that the spectral overlap does not required for energy transfer mechanism. This was also proven in our study that spectral overlap is not necessary between the absorption spectrum of a quencher and the emission spectrum of the donor (phthalocyanine).

Table 1. The name and structures of used quenchers and overlap graphics between absorption spectra of quenchers and emission spectrum of the peptide conjugated zinc(II) phthalocyanine (**5**). Concentration= $1.00x10^{-5}$.

Quencher	Quencher structure	$(Q)_{abs}$-$(PcP)_{ems}$
Q_1 *6-amino-quinoline* λ_{max}: 375	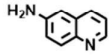	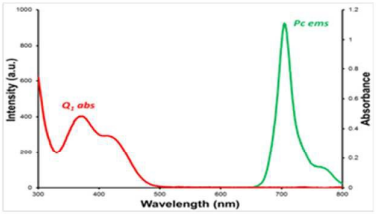
Q_2 *1-amino-pyrene* λ_{max}:390	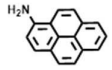	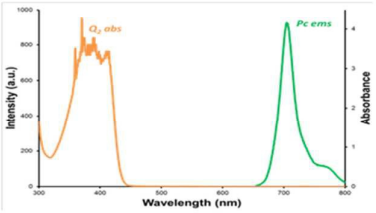
Q_3 *Atto-680®* λ_{max}:684	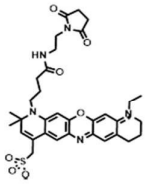	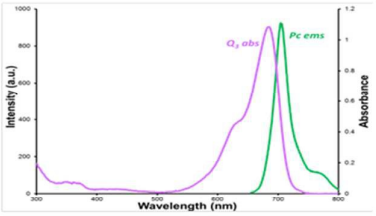
Q_4 *Phthalocyanine (**1**)* λ_{max}:686	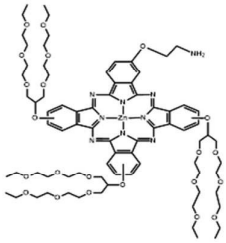	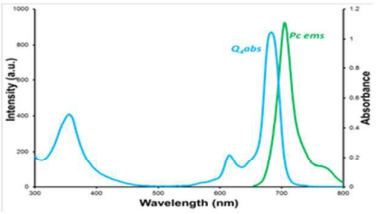

The absorption spectra of the quenchers and emission spectrum of the peptide conjugated Zn(II)Pc (**5**) were given in Table 1 and any spectral overlap did not show between

compound **5** and 6-aminoquinoline or 1-aminopyrene quenchers. On the other hand, an intense overlap was observed between compound **5** and Atto 680® or amino functionalized Pc quenchers. Our results show that overlap is not necessary for efficient quenching in the synthesized novel quenchers. In order to effective quenching, the energy levels of photosensitizer and quencher should be close.

3.6. Fluorescence quantum yields and lifetimes

Fluorescence consists when an orbital electron of a photosensitizer relaxes to its ground state by emitting a photon of light after being excited to a higher quantum state. The fluorescence quantum yield (Φ_F) value gives the efficiency of the fluorescence process. This value defined as the ratio of the number of photons emitted to the number of photons absorbed [36]. The Φ_F values of the studied conjugates (**6-9**) were ranged from 0.04 to 0.22 in DMSO (Table 2). These compounds showed very low Φ_F values as a result of energy transfer between phthalocyanine core and quencher except for conjugate **9**. The Φ_F value of the Pc-peptide conjugate (**5**) decreased approximately 80% by the substitution of quenchers for conjugates (**6**, **7** and **8**) due to energy transfer between Pc ring and quenchers. The beacon **9** which was formed conjugation of two Pc by peptide sequence showed higher Φ_F value than other molecular beacons (**6-8**). It suggested that energy transfer did not occur in this compound because donor and quencher groups were formed same Pc ring.

Another proof for the formation of energy transfer between Pc ring and quencher molecules was reducing the fluorescence lifetime (τ_F) value of peptide conjugated Zn(II)Pc compound (**5**) in DMSO after substitution of the different quenchers (Table 2).

Table 2. Photophysical and photochemical results of studied compounds in DMSO.

Compound	Φ_F	τ_F *ns*	Φ_Δ	Φ_d ($x10^{-5}$)
1[a]	0.22	2.11	0.711	1.53
2	0.26	3.28	0.697	2.53
5	0.16	4.08	0.46	2.53
6	0.09	1.83	0.14	1.05
7	0.06	1.22	0.16	2.46
8	0.04	1.33	0.17	1.54

9	0.22	1.91	0.32	1.04
***Std-ZnPc*[b]**	0.20	1.22	0.67	2.61

[a]Data from reference [30].

[b]Data from reference [34].

3.7. Singlet oxygen quantum yields

Singlet oxygen is formed from a bimolecular interaction between the triplet state of a photosensitizer and ground state (triplet) molecular oxygen. The amount of formed singlet oxygen is described as singlet oxygen quantum yield (Φ_Δ). The magnitude of singlet oxygen generation depends on the lifetime as well as energy of the photosensitizer molecules in the triplet state. There is a necessity of high efficiency of energy transfer between excited triplet state of photosensitizer and ground state of oxygen to generate large amounts of singlet oxygen for photochemical reactions [36].

The generated singlet oxygen by the studied compounds was determined using UV–vis. spectroscopy. The absorption decays of DPBF which is singlet oxygen scavenger during the light irradiation using photochemical set-up [36] were monitored at 417 nm (Fig 8 as an example for **9** in DMSO).

The Q band intensities of studied Zn(II)Pcs did not exhibit any changes during the light irradiation for singlet oxygen studies supporting that these compounds were not degraded during singlet oxygen measurements (Fig 8 as an example for compound **9**).

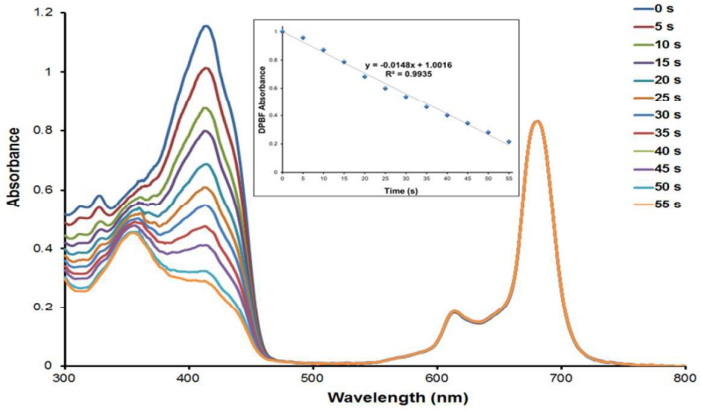

Figure 8. Absorbance changes during the determination of singlet oxygen quantum yield. This determination was for conjugate **9** in DMSO at a concentration of 1.0 x10^{-5} M. (Inset: Plot of DPBF absorbances versus irradiation time).

Table 2 shows that the singlet oxygen quantum yield values of conjugates (**6-9**) were found lower than starting Pc compounds (**1-3**) in DMSO due to energy transfer from

Pc ring to quencher molecules instead of molecular oxygen.

3.8. Photodegradation studies

Photodegradation studies are often conducted to establish the stability of phthalocyanine molecules on exposure to intense light and hence determine their efficacy for application in various fields. Photodegradation is a process where a molecule is degraded under light irradiation. It can be used to determinate stability of molecules and this is especially important for those molecules intended for use as photocatalysts [36].

The stabilities of newly synthesized carboxy-functionalized Zn(II)Pc (**2**), Pc-peptide conjugated derivative (**5**) and molecular beacons (**6-9**) were determined in DMSO by monitoring by decreasing in the intensity of the Q-band with increasing time under light irradiation (Fig. 9 for compound **6** as an example). The photodegradation quantum yield (Φ_d) values for the studied compounds (**1-9**) are listed in Table 2. The Φ_d values of the studied Pc (**1-9**) are order of 10^{-5} and similar Pc derivatives having different metals and substituents on the Pc ring giving in the literature [37]. The Φ_d values were reduced when the Pc-peptide conjugate attached with quenchers suggesting that the substitution of quenchers increased the stability of the studied Pc.

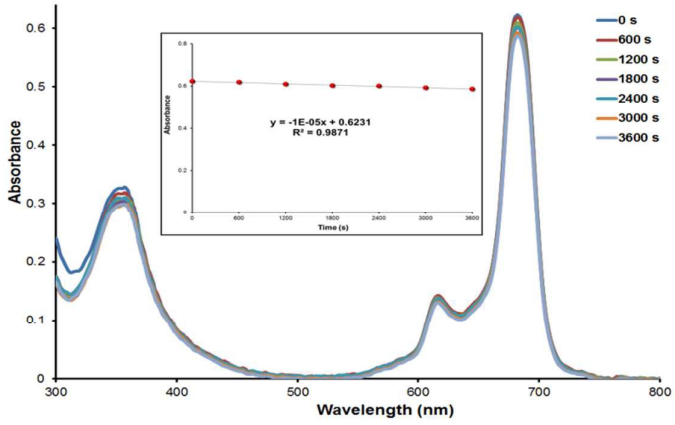

Figure 9. Absorbance changes during the photodegradation study of **6** in DMSO showing the decreasing of the Q and B bands at 10 minutes intervals (inset: plot of Q band absorbance versus time).

3.9. Cell Studies

The survival of HeLa cells following illumination with 1 J.cm^{-2} (data not shown) and 2 J.cm^{-2} of 680 nm (±10 nm) (Figure 10) light after uptake of the Pc **5** and conjugates **6-9** were

tested for determination of PDT activity of these photosensitizers *in vitro* medium. The cell survival percentages of studied photosensitizers were given in Table 3. Cell survival appears to be dose-dependent and any dark toxicity was not observed for all of the photosensitizers. These photosensitizers showed approximately 20% cell survival at concentration of 10 μM after 2 J.cm^{-2} irradiation except for conjugate **7** which it showed approximately 60% cell survival in the same conditions.

After treatment of 2 J.cm^{-2} irradiation with 2 μM, the cell survivals were found to be decreased by approximately 50% for **5**, **6** and **8** (Table 3). The cell survival was found 92% after treatment 2 J.cm^{-2} irradiation with 2 μM for conjugate **7**. This conjugate showed very limited PDT activity suggesting that the conjugation of 1-amino-pyren to Pc-peptide derivative was reduced photosensitizer efficiency. The conjugate **9** showed most activity with 24% cell survival at 2 J.cm^{-2} light irradiation against HeLa cells among the studied photosensitizers. As a result of the two-fold photosensitizer concentration in the cell culture was shown high cytotoxicity with conjugate **9.**

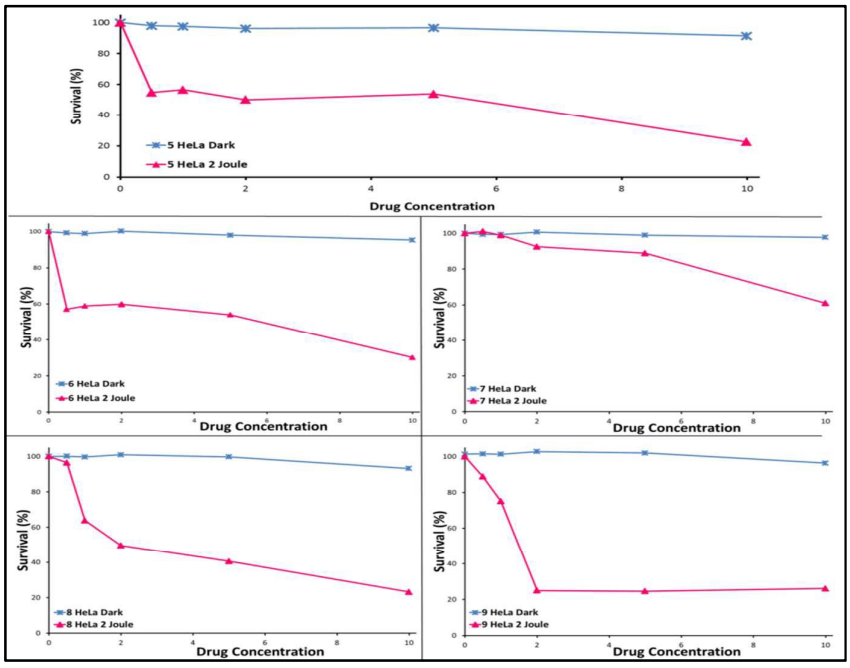

Figure 10. Survival of HeLa cells following illumination with 2 J.cm^{-2} of 680 nm (± 10 nm) light after 24 h with various concentration of Pc photosensitizers a) **5**, b) **6**, c) **7**, d) **8** and e) **9** administration. Each data represents the mean ± SD of three experiments.

Table 3. Percentage of HeLa cells survival following illumination with 2 J.cm^{-2} at 680 nm (± 10 nm) light after 24 hours incubation with various concentrations of photosensitizer molecules (**5**, **6, 7, 8,** and **9)**.

Concentration	Pc-Photosensitizers (survival, %)				
(μM)	**5**	**6**	**7**	**8**	**9**
0.5	54	57	101	96	88
1	56	58	98	63	75
2	50	59	92	49	*24*
5	53	53	88	40	*24*
10	*22*	*30*	61	*23*	*26*

On the other hand, the studied photosensitizers were added to exponentially growing cells and then incubated 24 hours for determination of fluorescence behavior of these photosensitizers. After this time, fluorescence re-occur in cell culture supernatant because of MMPs activity in HeLa cells. As a result that intramolecular energy transfer reduced by photoactivity of the molecules. Figure 11 shows the increasing of fluorescence intensities of studied photosensitizers (**5-9**) after MMP activity. These results show that the studied novel conjugate systems cleavage on the peptide sequence in the HeLa cells and fluorescence emissions of quenchers re-occur due to the formation of free quenchers in this cell media.

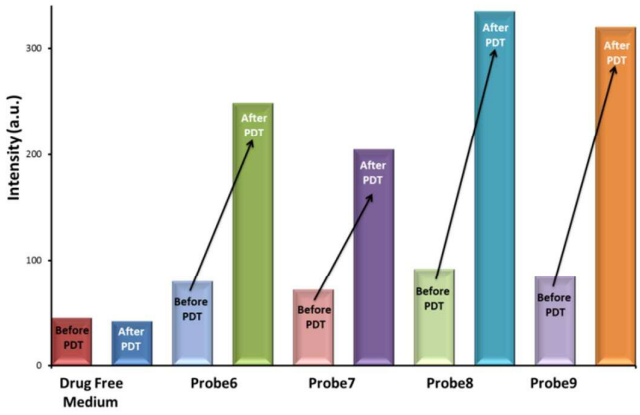

Figure 11. Fluorescence intensity of the cell culture supernatant, after treatment of conjugates (**6-9**) treatment.

The obtained photophysical and photochemical data such as singlet oxygen quantum yields (Φ_Δ), fluorescence quantum yields (Φ_F) and fluorescence lifetime (τ_F) were compared as % values in DMSO (Fig. 12). As shown in this figure, quite effective decreasing in these values after conjugation of the quencher to the Pc ring. These results provided that energy transfer was occurred between the Pc core and the quencher.

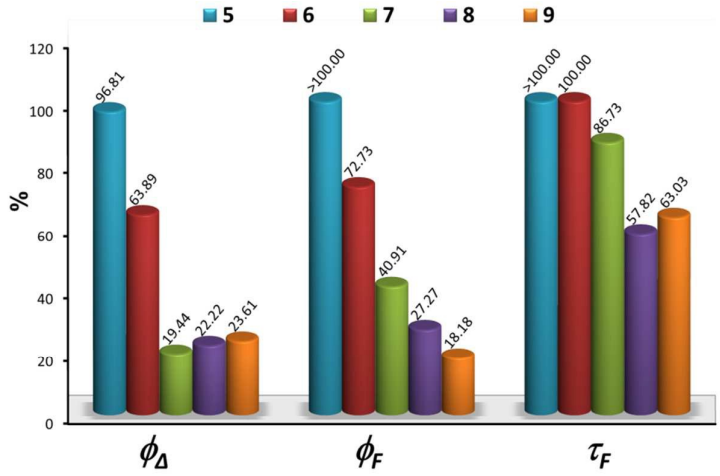

Figure 12. The comparison of the singlet oxygen quantum yield (Φ_Δ), fluorescence quantum yield (Φ_F) and fluorescence lifetime (τ_F) data as % values of novel conjugates (**6-9**) with starting Pc (**5**) in DMSO.

4. Conclusion

In this study, the synthesis of the novel Pc-peptide-quencher molecular beacons (**6-9**) were successfully achieved. These conjugates were characterized by standard methods including UV-vis, ^{1}H NMR, FT-IR, MALDI-TOF mass and elemental analysis as well. The photophysical and photochemical properties such as fluorescence quantum yields, lifetimes and singlet oxygen quantum yields of these conjugates were investigated in DMSO. In addition, the photodynamic activity of these conjugates (**6-9**) were tested against human HeLa cells. All these properties of novel conjugates were compared to the starting Pc (**5**). These conjugates were PDT inactive until reach the cancerous cells according to their photophysical and photochemical properties. It may be concluded that energy transfer between Pc ring and fluorophore group. These conjugates could be active in the cancer cells due to cleavage of peptide sequence by MMP enzymes in cancer cells. These MMP enzymes are secreted with limited level in the normal cells.

According to results, intramolecular energy transfer occurs in synthesized novel conjugates (**6-9**) and they could be passive until it reaches the target cancer tissue. Thus the synthesized novel conjugates may serve as activatable photosensitizers. They could be useful for non-toxic effect to healthy tissue and they could be exhibit good photodynamic activity in cancer cells.

References

1. M.R. Detty, S.L. Gibson, S.J. Wagner, *Journal of Medicinal Chemistry,* 2004, **47**, 3897;3915.
2. B. Turk, *Nat. Rev*., 2006, **5**, 785.
3. Law B., Tung C., *Bioconjug. Chem.*, 2009, **20,** 1683–1695.
4. M. Cicek, M.J. Oursler, *Cancer Metastasis Rev.,* 2006, **25,** 635–644.
5. R.L. Scherer, J.O. Mc Intyre, L.M. Matrisian, *Cancer Metastasis Rev.,* 2008, **27,** 679–690.
6. T.W. Liu, J. Chen, G. Zheng, *Amino Acids,* 2011, **41(2),** 1123-34.
7. C.E. Brinckerhoff, and L.M. Matrisian, *Nat. Rev. Mol. Cell Biol.,* 2002, **3,** 207–14.
8. T.A. Guise, *Genes Dev*., 2009, **23,** 2117–23.
9. M. Ii, H. Yamamoto, Y. Adachi, Y. Maruyama, Y. Shinomura, *Exp Biol Med*., 2006, **231,** 20–27.
10. K. Kessenbrock, V. Plaks, and Z. Werb, *Cell,* 2010, **141,** 52-67.
11. C.H. Tung, *Biopolymers*, 2004, **76,** 391–403.
12. T. Jiang, E. S. Olson, Q. T. Nguyen, M. Roy, P. A. Jennings and R. Y. Tsien, Proc. Natl. Acad. Sci. U. S. A., 2004, **101**, 17867–17872.
13. E. A. Goun, R. Shinde, K. W. Dehnert, A. Adams-Bond, P. A. Wender, C. H. Contag and B. L. Franc, Bioconjugate Chem., 2006, **17**, 787–796.
14. G. Blum, S. R. Mullins, K. Keren, M. Fonovic, C. Jedeszko, M. J. Rice, B. F. Sloane and M. Bogyo, Nat. Chem. Biol., 2005, **1**, 203–209.
15. D. Kato, K. M. Boatright, A. B. Berger, T. Nazif, G. Blum, C. Ryan, K. A. Chehade, G. S. Salvesen and M. Bogyo, Nat. Chem. Biol., 2005, **1**, 33–38.
16. G. Blum, G. von Degenfeld, M. J. Merchant, H. M. Blau and M. Bogyo, Nat. Chem. Biol., 2007, **3**, 668–677.
17. M.Verhille, H. Benachour, A. Ibrahim, M. Achard, P. Arnoux, M. Barberi-Heyob, J.C. Andre, X. Allonas, F. Baros, R. Vanderesse, C. Frochot, Curr. Med. Chem., 2012, **19**, 5580-5594.
18. M. Verhille, P. Couleaud, R. Vanderesse, D. Brault, M. Barberi-Heyob, C. Frochot, Current Medicinal Chemistry, 2010, **17**, 3925-3943.
19. J. Chen, K. Stefflova, M.J. Niedre, B.C. Wilson, B. Chance, J.D. Glickson, G. Zheng, J. Am. Chem. Soc., 2004, **126**, (37), 11450-11451.
20. G. Zheng, J. Chen, K. Stefflova, M. Jarvi, H. Li, B.C. Wilson, PNAS, 2007, **104**, (21), 8989-8994.

21. J. Chen, K. Stefflova, M. Warren, J. Bu, B.C. Wilson, G. Zheng, Proc. SPIE Int. Soc. Opt. Eng., 2007, 6449, (Genetically Engineered and Optical Probes for Biomedical Applications IV), 1-9.
22. P. Lo, J. Chen, K. Stefflova, M.S. Warren, R. Navab, B. Bandarchi, S. Mullins, M. Tsao, J.D. Cheng, G. Zheng, J. Med. Chem., 2009, **52**, (2), 358-368.
23. J.F. Lovell, T.W.B. Liu, J. Chen, and G. Zheng, Chem. Rev., 2010, **110**, 2839–2857.
24. S. Lee, K. Park, K. Kim, K. Choi and I.C. Kwon, *Chem. Commun.,* 2008, 4250-4260.
25. B. Ballou et al., *Cancer Immunol. Immunother.,* 1995, **41,** 257-263.
26. K. Licha et al., *Photochem. Photobiol.,* 2000, **72,** 392-398.
27. A. Becker, et al., *Photochem. Photobiol.,* 2000, **72,** 234-241.
28. R. Weissleder, C.H. Tung, U. Mahmood & A.Jr. Bogdanov, *Nat. Biotechnol*., 1999, **17,** 375-378.
29. A. Becker, C. Hessenius, K. Licha, B. Ebert, U. Sukowski, W. Semmler, B. Wiedenmann, and C. Grötzinger, *Nature Biotechnology*, 2001, **19,** 327-331.
30. M. Göksel, M. Durmuş, D. Atilla*, Journal of Photochemistry and Photobiology A: Chemistry,* 2013, **266,** 37– 46.
31. M. Sibrian-Vazquez, J. Ortiz, I.V. Nesterova, F. Fernandez-Lazaro, A. Sastre-Santos, S.A. Soper, M.G.H. Vicente, *Bioconjugate Chem*., 2007, **18,** 410-420.
32. R.B. Merrifield, *J. Am. Chem. Soc.,* 1963, **85(14),** 2149–2154.
33. M.J. Stillman, T. Nyokong, in: C.C. Leznoff, A.B.P. Lever, (Eds.), Phthalocyanines: Properties and Applications, vol. 1, VCH Publishers, New York, 1989 (Chapter 3).
34. I. Gürol, M. Durmuş, V. Ahsen, T. Nyokong, *Dalton Transactions*, 2007, **34,** 3782–3791.
35. J.F. Lovell, J. Chen, M.T. Jarvi, W. Cao, A.D. Allen, Y. Liu, T.T. Tidwell, BC. Wilson, G. Zheng, *J. Phys. Chem. B*, 2009, **113,** 3203-3211.
36. M. Durmuş, Photochemical and photophysical characterization, in T. Nyokong, V. Ahsen (Eds.), Photosensitizers in Medicine, Environment, and Security, Springer, New York, 2012, pp. 135-267.
37. T. Nyokong, Effects of substituents on the photochemical and photophysical properties of main group metal phthalocyanines, Coord. Chem. Rev. 251 (2007) 1707-1722.

Graphical abstract

Activatable molecular beacons were synthesized bearing phthalocyanine, peptide sequence and fluorofophor groups. The phototoxicity and cytotoxicity of the systems were studied against cervical cancer cell line named HeLa for their evaluation of the suitability for photodynamic therapy.